Semicond. Sci. Technol. 8 (1993) S62–S65. Printed in the UK

Infrared photoluminescence on molecular beam epitaxially grown $Hg_{1-x}Cd_xTe$ layers

M M Kraus, C R Becker, S Scholl, Y S Wu, S Yuan and G Landwehr

Physikalisches Institut der Universität Würzburg, D-8700 Würzburg, Federal Republic of Germany

Abstract. $Hg_{1-x}Cd_xTe$ is an important material for infrared device technology. Despite a variety of investigations on molecular beam epitaxially (MBE) grown Hg-based superlattices and modulation-doped structures, little attention has been paid to the study of the photoluminescence properties of the constituent materials. We report here on a systematic study of infrared photoluminescence on $Hg_{1-x}Cd_xTe$ layers grown by MBE. The Fourier transform photoluminescence of $Hg_{1-x}Cd_xTe$ layers with $0.25 < x < 0.93$ grown on (110) and (211) GaAs was investigated in the spectral range from 0.1 eV to 1.5 eV. Emission lines were observed with a full width at half maximum down to 15 meV. Photoluminescence and transmission properties are compared over the temperature range from 4.2 K to 300 K. The possible influences of Burstein–Moss shift, impurity bands and exponential band tails are discussed. Photoluminescence at high temperatures originates from band-to-band transitions. However, low temperature photoluminecence can be attributed either to impurity bands or to additional states due to band tails.

1. Introduction

$Hg_{1-x}Cd_xTe$ can be considered to be the state-of-the-art material for infrared detection technology. A substantial part of the experimental effort to understand and improve the properties of this material was focused on electrical methods [1, 2]. Many of the optical investigations to date have been transmission experiments which were performed in order to study effects of band tails in this ternary alloy system [3, 4]. The photoluminescence of $Hg_{1-x}Cd_xTe$ was first measured by Elliot *et al* [5] more than 20 years ago. From the observation of two emission lines the high energy line was attributed to band–band recombination while the low energy line was assigned to electron–acceptor transitions.

In this work, the photoluminescence properties of thin molecular beam epitaxially grown $Hg_{1-x}Cd_xTe$ layers were investigated. Additional transmission experiments were performed to reveal the position of the emission lines with respect to the bandgap. The photoluminescence spectra are explained by taking into account the exponential band tails dominant in ternary systems with varying degrees of disorder.

2. Experiment

Epitaxial growth of the $Hg_{1-x}Cd_xTe$ layers was performed in a four-chamber Riber 2300 molecular beam epitaxial (MBE) system, modified to permit the growth of Hg-based materials. Details of the growth are described by He *et al* [6]. The thickness of the layers was in the range from 4 to 9 μm. The infrared photoluminescence and transmission were measured with a commercial Bruker IFS88 FTIR spectrometer, which has been altered to enable the collection of luminescence light. A KBr beamsplitter was used along with a mercury cadmium telluride MCT detector cooled to 77 K. A Nd:YAG laser was employed as the excitation source. The excitation power density was in the range 1 to 2 W cm^{-2}. In order to separate the weak photoluminescence light from the dominant background radiation, a double modulation technique was used with phase-sensitive detection. The lower detection limit of 100 meV was imposed by the cut-off energy of the MCT detector. The samples were mounted in a helium gas-exchange cryostat equipped with ZnSe windows and cooled to temperatures ranging from 4.2 to 300 K.

3. Results

The 4.2 K photoluminescence spectra of four selected $Hg_{1-x}Cd_xTe$ layers are shown in figure 1 and a survey of all the layers investigated with x-values in the range 0.25–0.93 is given in figure 2.

0268-1242/92/010S62+04$07.50

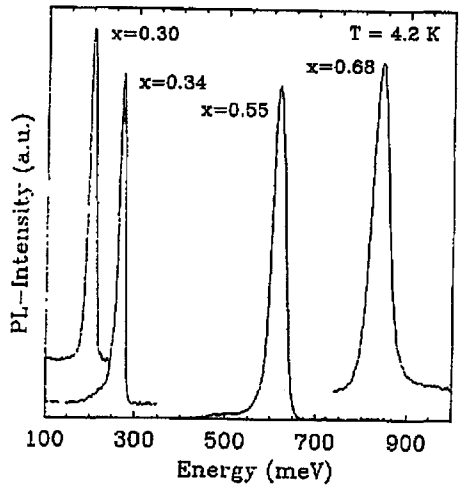

Figure 1. Photoluminescence of four $Hg_{1-x}Cd_xTe$ layers at a temperature of 4.2 K. The scale is arbitrary.

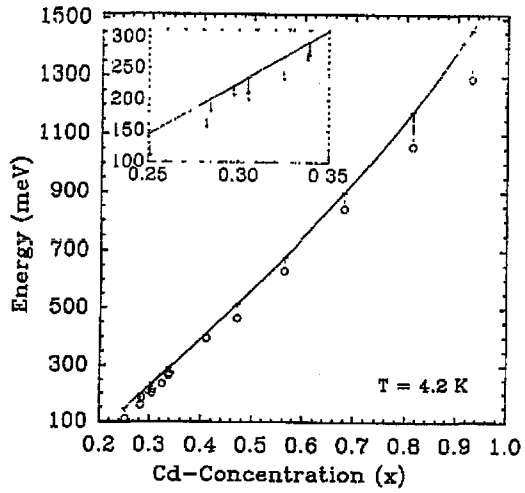

Figure 2. Survey of all $Hg_{1-x}Cd_xTe$ layers investigated. The quasi-diagonal line denotes the relationship between energy gap and x-value according to Hansen *et al* [7]. The vertical lines correspond to the energy difference between the onset of the photoluminescence and its maximum and schematically represent the linewidth of the emission. For clarity the range $0.25 < x < 0.35$ is enlarged in the inset.

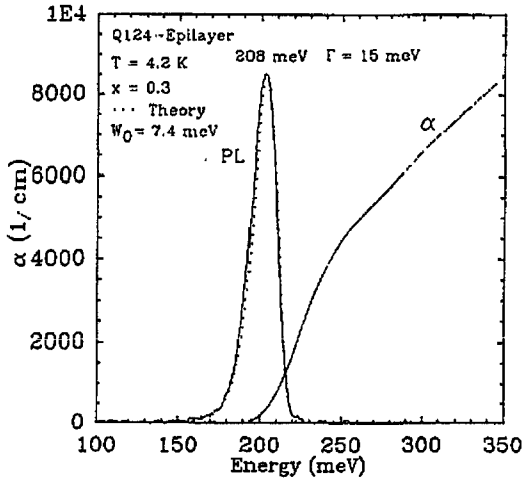

Figure 3. 4.2 K photoluminescence and absorption at 4.2 K of $Hg_{0.7}Cd_{0.3}Te$. The dotted curve is the result of a theoretical lineshape calculation with an effective carrier temperature of T_{eff} =20 K.

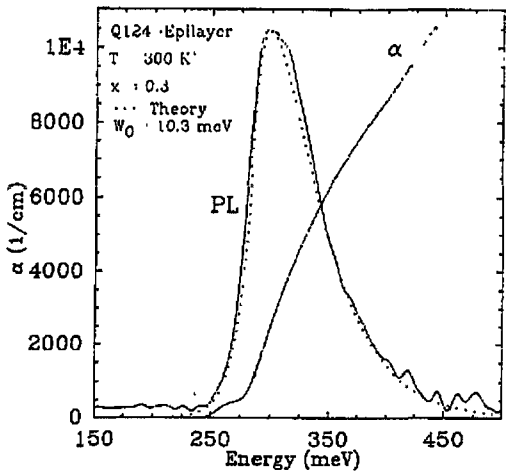

Figure 4. Photoluminescence and absorption of $Hg_{0.7}Cd_{0.3}Te$ at 300 K. The dotted curve represents the numerical result with an effective carrier temperature of T_{eff} =360 K.

Each spectrum in figure 1 is dominated by a single emission line. Depending on the composition of the layers, the photoluminescence lines cover a wide spectral range from the mid-infrared to the near-infrared [7]. The full width at half maximum (FWHM) of the emission lines increases with x-value from 15 to 43 meV. The narrowest line was obtained from the sample with $x = 0.3$. The corresponding spectrum with its peak at an energy of 208 meV and a FWHM of 15 meV is shown together with the approximate absorption coefficient α as determined by transmission in figure 3. Clearly it can be seen that the majority of the emission occurs in the spectral range well below the $\alpha = 1000\ cm^{-1}$ point, which according to convention is defined as the bandgap [3]. The corresponding data for 300 K are shown in figure 4. In this case the low energy emission coincides with the onset of absorption. As the temperature is increased, the photoluminescene is shifted closer to the absorption edge. At low temperatures, the onset of the absorption is found on the high energy side of the photoluminescence. In contrast, the photoluminescence is located above the absorption edge at higher temperatures. This behaviour was found to be typical of all the samples investigated.

4. Discussion

For all high-quality MBE samples investigated a single and rather broad emission line was observed. The increase of linewidth with increasing x-value is consistent with the effects of alloy broadening [8]. Due to the decrease in the effective electron mass with decreasing bandgap [9], the maximum contribution to alloy broadening is shifted from x=0.5 to higher x-values. Although the photoluminescence lines are very narrow for MBE-grown material, all the linewidths are larger by a factor of 2 to 3 than the linewidths for good bulk

$Hg_{1-x}Cd_xTe$ [10–12]. MBE growth is carried out far from thermal equilibrium at rather low substrate temperatures, e. g. 180 °C, which are necessary to grow Hg-containing material. This may favour compositional fluctuations in excess of the minimum statistical fluctuations [8] and could thus account for the enlarged linewidths.

In comparison with the transmission data, most of the photoluminescence at 4.2 K was below the corresponding absorption edge. Therefore we conclude that the observed low temperature emission does not arise from band-to-band transitions as suggested by Elliot *et al* [5] and other authors [10, 13–15] but rather from recombination through states located in the fundamental bandgap of the material, as is the case for $Cd_{1-x}Mn_xTe$ and binary semiconductors.

For the correct interpretation of the photoluminescence, both the transmission and the electrical properties have to be considered. All the layers investigated were as-grown n-type with typical carrier concentrations in the low 10^{16} cm^{-3} range at 4.2 K. In this regime, substantial band filling could be expected due to the small effective electron mass [16]. The shift of the Fermi energy into the conduction band could then cause a blue shift of the absorption edge (Burstein–Moss shift) [17]. On the other hand, poor sample quality with dominating defect bands could also lead to emission below the bandgap. In order to exclude these principal possiblities, both photoluminescence and transmission were measured on high-quality bulk p-type $Hg_{1-x}Cd_xTe$, from which both defect bands and band filling should be absent. Here the same characteristic relationship between photoluminescence and transmission was observed [18]. Another possible source of the photoluminescence is due to an additional density-of-states tail in the forbidden energy gap of $Hg_{1-x}Cd_xTe$, whose existence has been demonstrated in a number of experiments [3, 12, 19, 20]. Following the concept of Cohen *et al* [21], the absorption in this region is usually [12, 22, 23] described as

$$\alpha_{tail} = \alpha_0 \exp\left(\frac{E - E_0}{W_0}\right) \tag{1}$$

where W_0 denotes the strength of the band tail and E_0 marks the transition energy between the Kane absorption as described by Anderson [24] and the additional tail. Typically the values for W_0 range from 2 to 10 meV [3, 4, 22]. To obtain the position of the Fermi energy, both the magnitude of the density of states due to the tail and the measured carrier concentration have to be considered. The well known Fermi integral formalism for parabolic bands [25] can be extended in order to account qualitatively for the additional density of states below the bandgap:

$$n_0 = \frac{N_c}{\Gamma_{3/2}}\left(\int_{-\infty}^{\epsilon_t} \frac{\sqrt{\epsilon_t}\exp\left(\frac{\epsilon-\epsilon_t}{2\epsilon_t}\right)\mathrm{d}\epsilon}{1+\exp(\epsilon-\eta)} + \int_{\epsilon_t}^{\infty} \frac{\sqrt{\epsilon}\,\mathrm{d}\epsilon}{1+\exp(\epsilon-\eta)}\right) = N_c F_{1/2}^{tail} \tag{2}$$

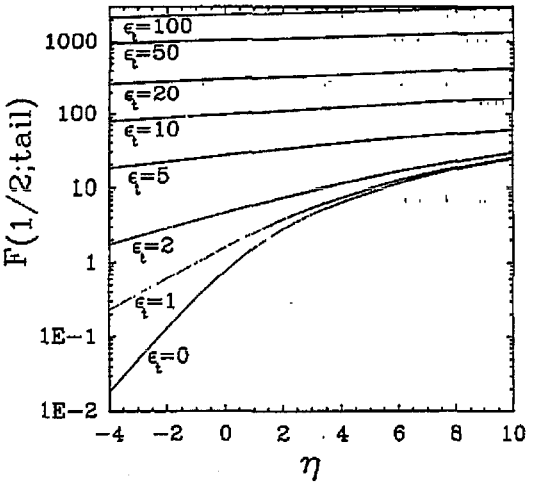

Figure 5. Integral over the quasi-Fermi integral given in equation (2) for different values of the dimensionless quantity ϵ_t which describes the strength of the exponential tail.

The effect of an additional density of states due to the tail with $\epsilon_t = W_0/2kT$ as a variable parameter is shown in figure 5. Assuming for example that the reduced Fermi energy η is located at the bottom edge of the conduction band ($\eta = 0$), $F_{1/2}^{tail}$ has a value of approximately 1 if tail effects are absent ($\epsilon_t = 0$). The corresponding carrier concentration is then given by N_c. A much higher carrier concentration is possible if ϵ_t is assumed to have a value of 10. In this case the carrier concentration can be larger by two orders of magnitude without moving the Fermi energy into the band. From this one can see that a high carrier concentration does not shift the Fermi energy into the conduction band if band tails are allowed. Therefore the classical band filling phenomena should be negligible, especially in cases where ϵ_t is large. This is the case for MBE-grown $Hg_{1-x}Cd_xTe$. Qualitatively the same effect could be caused by impurity bands, which are to be expected above a critical carrier concentration as low as $n_{crit} \approx 5.5 \times 10^{14}$ cm^{-3} [26] for $x = 0.3$ material.

The exponential behaviour of α also plays a key role in the numerical simulation of the photoluminescence lineshape. Following the concept developed by Herrmann *et al* [12] and employing the notation given by Anderson [27], the spontaneous photoluminescence is described by

$$r_{spont}(E) = \frac{n^2E^2}{\pi^2c^2\hbar^2}\frac{\alpha}{\exp\left(\frac{E-E_g-Q_n-Q_p}{kT}\right)-1}. \tag{3}$$

$E = \hbar\omega$ is the quantum energy and E_g is the energy gap. The two quasi-Fermi energies Q_n and Q_p for electrons and holes are positive if they are located in the conduction or valence band respectively. In our calculations the values for both Q_n and Q_p had to be selected in the range from -5 to -10 meV in order to fit the experimental data. Here the absorption coefficient α as given by Anderson [24] and modified to include band tails was employed. The factor α_0 was chosen to ensure continuity of both the absorption coefficient and

its derivative at the transition point E_0. The results of these calculations are included in figures 3 and 4 (dotted curves). For the 4.2 K spectrum in figure 3, a tail parameter of 7.4 meV had to be used, which is considerably larger than other low-temperature values for bulk material [3, 4, 22]. The value scales approximately with the enlarged FWHM and indicates that permanent broadening mechanisms are present in the MBE samples investigated as a result of the non-equilibrium nature of the MBE growth. At 300 K we obtained a tail parameter of 10.3 meV (figure 3). This is also larger than values found in bulk material at this temperature. However, the phonon-activated enhancement of this quantity compares well with the results on bulk material [18, 22].

A comparison of figures 3 and 4 shows that this model can describe both the low and high temperature photoluminescence. At low temperatures however, the emission occurs mainly in the spectral region that is assigned to an exponential tail. Due to thermal effects, the room temperature emission follows mainly the Kane-like absorption.

5. Conclusion

From a systematic comparison of photoluminescene and transmission properties of MBE grown $Hg_{1-x}Cd_xTe$ layers we conclude that the photoluminescence properties over a wide range of temperature can be described by a model taking into account exponential band tails. This model accurately predicts the photoluminescence lineshape. At low temperatures photoluminescence arises from states in an exponential tail, i.e. in the fundamental bandgap. Significant contributions from states within the conventional conduction or valence bands are observed only at higher temperatures.

Acknowledgments

This project was supported by the Bundesministerium für Forschung und Technologie (BMFT).

References

[1] Capper P 1989 *Prog. Crystal Growth Charact.* **19** 295
[2] Hoerstel W, Klimakow A and Kramer R 1990 *J. Crystal Growth* **101** 854
[3] Finkman E and Nemirovsky Y 1979 *J. Appl. Phys.* **50** 4356
[4] Finkman E and S Schacham E 1984 *J. Appl. Phys.* **56** 2896
[5] Elliot C T, Melngailis I, Harman T C and Foyt A G 1989 *J. Phys. Chem. Solids* **33** 1527
[6] He L, Becker C R, Bicknell-Tassius R N, Scholl S and Landwehr G 1993 *Semicond. Sci. Technol.* **8** S216
[7] Hansen G L, Schmit J L and Casselman T N 1982 *J. Appl. Phys.* **53** 7099
[8] Schubert E F, Göbel E O, Horikoshi, Ploog K and Queisser H J 1984 *Phys. Rev.* B **30** 813
[9] Osbourn G C and Smith D L 1979 *Phys. Rev.* B **20** 1556
[10] Hunter A T and McG ill T C 1981 *J. Appl. Phys.* **52** 5779
[11] Lusson A, Fuchs F and Marfaing Y 1990 *J. Crystal Growth* **101** 673
[12] Herrmann K H, Möllmann K P and Tomm J W 1992 *J. Crystal Growth* **117** 758
[13] Ivanov-Omskii V I, Maltseva V A, Briov A D and Sivachenko S D 1978 *Phys. Status Solidi* a **46** 77
[14] Hunter A T, Smith D L and McGill T C 1980 *Appl. Phys. Lett.* **37** 200
[15] Hunter A T and McGill T C 1982 *J. Vac. Sci. Technol.* **21** 205
[16] Brice J and Capper P (ed) 1987 *Properties of Mercury Cadmium Telluride* EMIS Datareviews Series No 3 (New York: INSPEC)
[17] Pankove J I 1971 *Optical Processes in Semiconductors* (New York: Dover)
[18] submitted to *J. Appl. Phys.*
[19] Hougen C A 1989 *J. Appl. Phys.* **66** 3763
[20] Maxey C D, Capper P, Easton B C and Whiffin P A C 1989 *Infrared Physics* **29** 961
[21] Cohen E and Sturge M D 1982 *Phys. Rev.* B **25** 3828
[22] Herrmann K H, Jank U and Möllmann K P 1989 *Phys. Status Solidi* a **114** K249
[23] Fuchs F and Koidl P 1991 *Semicond. Sci. Technol.* **6** C76
[24] Anderson W W 1980 *Infrared Physics* **20** 363
[25] Blakemore J S 1962 *Semiconductor Statistics* (New York: Pergamon)
[26] Stern F and Dixon J R 1959 *J. Appl. Phys.* **30** 268
[27] Anderson W W 1977 *IEEE J. Quantum Electron.* **13** 532